$Rb_4Hg_5(Te_2)_2(Te_3)_2Te_3$, $[Zn(en)_3]_4In_{16}(Te_2)_4(Te_3)Te_{22}$, and $K_2Cu_2(Te_2)(Te_3)$: Novel Metal Polytellurides with Unusual Metal−Tellurium Coordination

Xuean Chen, Xiaoying Huang, and Jing Li*

Department of Chemistry, Rutgers University, Camden, New Jersey 08102

Received June 15, 2000

Three novel metal polytellurides $Rb_4Hg_5(Te_2)_2(Te_3)_2Te_3$ (**I**), $[Zn(en)_3]_4In_{16}(Te_2)_4(Te_3)Te_{22}$ (**II**), and $K_2Cu_2(Te_2)(Te_3)$ (**III**) have been prepared by solvothermal reactions in superheated ethylenediamine at 160 °C. Their crystal structures have been determined by single-crystal X-ray diffraction techniques. Crystal data for **I**: space group *Pnma*, $a = 9.803(2)$ Å, $b = 9.124(2)$ Å, $c = 34.714(7)$ Å, $Z = 4$. Crystal data for **II**: space group *C2/c*, $a = 36.814(7)$ Å, $b = 16.908(3)$ Å, $c = 25.302(5)$ Å, $\beta = 128.46(3)°$, $Z = 4$. Crystal data for **III**: space group *Cmcm*, $a = 11.386(2)$ Å, $b = 7.756(2)$ Å, $c = 11.985(2)$ Å, $Z = 4$. The crystal structure of **I** consists of 1D infinite ribbons of $^1_\infty[Hg_5(Te_2)_2(Te_3)_2Te_3]^{4-}$, which are composed of tetrahedral $HgTe_4$ and trigonal $HgTe_3$ units connected through the bridging Te^{2-}, $(Te_2)^{2-}$, and $(Te_3)^{2-}$ ligands. **II** is a layered compound containing $InTe_4$ tetrahedra that share corners and edges via Te, Te_2, and Te_3 units to form a 2D slab that contains relatively large voids. The $[Zn(en)_3]^{2+}$ template cations are filled in these voids and between the slabs. The primary building blocks of **III** are $CuTe_4$ tetrahedra that are linked by intralayer $(Te_3)^{2-}$ and interlayer $(Te_2)^{2-}$ units to form a 3D network with open channels that are occupied by the K^+ cations. All three compounds are rare polytelluride products of solvothermal reactions that contain both Te_2 and Te_3 fragments with unusual metal−tellurium coordination.

Introduction

A tremendous amount of research has been conducted on solid-state telluride compounds over the past decade. The molten alkali-metal polychalcogenide flux growth technique has proven to be an effective method for the syntheses of metal polytellurides with long terminal or bridging $(Te_x)^{2-}$ ($x \geq 2$) units as their characteristic building blocks.[1] In contrast, solvothermal reactions often produce monotellurides composed of corner- or edge-sharing MTe_x ($x = 3-6$) polyhedra,[2] with exceptions of several binary polytellurides containing long $(Te_x)^{2-}$ fragments. These include the Te_4^{2-}, Te_6^{2-}, and Te_{13}^{2-} units found in $[Mn(en)_3]Te_4$ (en = ethylenediame)[3,4] Cs_4Te_{28}, and Cs_2Te_{13},[5] respectively; the 2D $^2_\infty[Te_6^-]$ network present in $RbTe_6$;[6] the $^2_\infty[Te_6]^{3n-}$ planar nets and crown-shaped Te_8 rings observed in Cs_3Te_{22};[7] and a 3D $^3_\infty[Te_6]^{3n-}$ framework structure encountered in $[Cr(en)_3]Te_6$.[8] Only a relatively small number of ternary phases contain polytelluride Te_x^{2-} fragments, and they are usually restricted to $x = 2$, as exemplified by the Te_2^{2-} fragments in $Cs_4As_2(Te_2)_2(Te)_2$,[9] $A_2M(Te_2)(Te)_2$ (A = K, Cs; M = Ge, Sn),[10,11] $[M(en)_3]In_2(Te_2)_2Te_2$ (M = Fe, Zn), and α,β-$[Mo_3(en)_3(Te_2)_3(O)(Te)]In_2(Te_2)_2Te_2$.[12] In this paper, we report three new ternary polytellurides: $Rb_4Hg_5(Te_2)_2(Te_3)_2Te_3$ (**I**), $[Zn(en)_3]_4In_{16}(Te_2)_4(Te_3)Te_{22}$ (**II**), and $K_2Cu_2(Te_2)(Te_3)$ (**III**), whose structures range from extended 1D ribbon to 3D framework and are all characterized by the presence of both Te_2 and Te_3 units with interesting and unusual bonding modes.

Experimental Section

Materials. A_2Te (A = K, Rb) compounds were prepared by reactions of alkali metal and elemental Te in a 2:1 ratio in liquid ammonia. HgTe and $TiTe_2$ were prepared by stoichiometric reactions of elements at 200 and 450 °C, respectively. The other chemicals were used as purchased without further treatment: $InCl_3$ (99.5%, Fisher Scientific), $ZnCl_2$ (99.5%, Fisher), CuCl (99%, Aldrich), Bi_2Te_3 (99%, Alfa), Te (99.5%, Strem Chemicals, Inc.), and ethylenediamine (99%, anhydrous, Aldrich).

Synthesis. $Rb_4Hg_5(Te_2)_2(Te_3)_2Te_3$ (**I**) was prepared by weighing and mixing 0.075 g (0.25 mmol) of Rb_2Te, 0.100 g (0.25 mmol) of Bi_2Te_3, 0.082 g (0.25 mmol) of HgTe, and 0.096 g (0.75 mmol) of Te in a glovebox under an inert atmosphere of argon. The mixture was then transferred to a thick-walled Pyrex tube, and 0.37 mL of en was added to it. After the liquid was condensed by liquid nitrogen, the tube was sealed with a torch under a vacuum of $\sim 10^{-3}$ Torr. The sample was placed in an oven and heated at 160 °C for 1 week. The gray, needlelike crystals in about 20% yield were isolated by washing the reaction product with 20% and 80% ethanol followed by drying with anhydrous diethyl ether. The remaining product was identified by powder X-ray diffraction to be mainly Bi_2Te_3.

$[Zn(en)_3]_4In_{16}(Te_2)_4(Te_3)Te_{22}$ (**II**) was synthesized from a reaction of 0.034 g (0.25 mmol)og $ZnCl_2$, 0.150 g (0.75 mmol) of $InCl_3$, and 0.224 g (1.75 mmol) of Te, while single crystals of $K_2Cu_2(Te_2)(Te_3)$ (**III**) were grown from reactions containing 0.052 g (0.25 mmol) of K_2Te, 0.075 g (0.25 mmol) of $TiTe_2$, 0.025 g (0.25 mmol) of CuCl,

* To whom correspondence should be addressed.

(1) Kanatzidis, M. G.; Sutorik, A. C. *Prog. Inorg. Chem.* **1995**, *43*, 151.
(2) Sheldrick, W. S.; Wachhold, M. *Angew. Chem., Int. Ed. Engl.* **1997**, *36*, 206.
(3) Wendland, F.; Näther, C.; Bensch, W. *Z. Anorg. Allg. Chem.* **2000**, *626*, 456.
(4) Li, J.; Chen, Z.; Wang, R.-J.; Proserpio, D. M. *Coord. Chem. Rev.* **1999**, *190−192*, 707.
(5) Sheldrick, W. S.; Wachhold, M. *Chem. Commun.* **1996**, 607.
(6) Sheldrick, W. S.; Schaaf, B. *Z. Naturforsch.* **1994**, *49b*, 993.
(7) Sheldrick, W. S.; Wachhold, M. *Angew. Chem., Int. Ed. Engl.* **1995**, *34*, 450.
(8) Reisner, C.; Tremel, W. *Chem. Commun.* **1997**, 387.
(9) Wachhold, M.; Sheldrick, W. S. *Z. Naturforsch.* **1996**, *51b*, 1235.
(10) Sheldrick, W. S.; Schaaf, B. *Z. Naturforsch.* **1994**, *50b*, 1469.
(11) Sheldrick, W. S.; Schaaf, B. *Z. Naturforsch.* **1994**, *49b*, 57.
(12) Li, J.; Chen, Z.; Emge, T. J.; Proserpio, D. M. *Inorg. Chem.* **1997**, *36*, 1437.

10.1021/ic000648c CCC: $20.00
Published on Web 02/07/2001

Table 1. Crystallographic Data for $Rb_4Hg_5(Te_2)_2(Te_3)_2Te_3$ (**I**), $[Zn(en)_3]_4In_{16}(Te_2)_4(Te_3)Te_{22}$ (**II**), and $K_2Cu_2(Te_2)(Te_3)$ (**III**)

	I	II	III
formula	$Rb_4Hg_5(Te_2)_2(Te_3)_2Te_3$	$[Zn(en)_3]_4In_{16}(Te_2)_4(Te_3)Te_{22}$	$K_2Cu_2(Te_2)(Te_3)$
fw	3003.63	7030.64	843.28
space group	*Pnma* (No. 62)	*C2/c* (No. 15)	*Cmcm* (No. 63)
a, Å	9.803(2)	36.814(7)	11.386(2)
b, Å	9.124(2)	16.908(3)	7.756(2)
c, Å	34.714(7)	25.302(5)	11.985(2)
α, deg	90	90	90
β, deg	90	128.46(3)	90
γ, deg	90	90	90
V, Å^3	3104.9(11)	12332(4)	1058.4(4)
Z	4	4	4
temp, °C	293	293	293
d_{calcd}, g/cm^3	6.425	3.787	5.292
λ, Å	0.710 73	0.710 73	0.710 73
μ, cm^{-1}	4.2833	1.1372	1.8239
R1 [$I \geq 2\sigma(I)$][a]	0.0423	0.0739	0.0317
wR2 (all data)[b]	0.0785	0.1089	0.0686

[a] $R1 = \sum||F_o| - |F_c||/\sum|F_o|$. [b] $wR2 = \{\sum[w(F_o^2 - F_c^2)^2]/[\sum w(F_o^2)^2]\}^{1/2}$.

and 0.096 g (0.75 mmol) of Te. The heating and isolation procedures for both compounds were the same as previously described for **I**. The black platelike crystals of **II** in about 30% yield and black rock crystals of **III** in about 10% yield were obtained from their respective reaction products. The byproduct accompanying **II** was unreacted Te, and the byproducts were Te and a binary phase $TiTe_2$ in the case of **III**. All three compounds appeared to be relatively stable in air and water.

Crystal Structure Determination. Intensity data of the title compounds were collected at room temperature (293 ± 1 K) on an Enraf-Nonius CAD4 automatic four-circle diffractometer with graphite monochromated Mo Kα radiation. Cell dimensions were obtained from least-squares refinements with 25 automatically centered reflections in the ranges $9.63° \leq \theta \leq 13.86°$ (**I**), $5.21° \leq \theta \leq 13.57°$ (**II**), and $9.70° \leq \theta \leq 19.29°$ (**III**). Three standard reflections were remeasured after every 2 h. No decay was observed except the statistic fluctuation in the range of ±2.3% (**I**), ±5.3% (**II**), and ±2.3% (**III**). Raw intensities were corrected for Lorentz and polarization effects and for absorption by an empirical method based on *ψ*-scan data. Direct phase determination and subsequent difference Fourier map synthesis yielded the positions of all non-hydrogen atoms, all of which were eventually subjected to anisotropic refinements except the carbon atoms in **II,** which were refined isotropically. Hydrogen atoms in **II** were placed at calculated positions, and their isotropic thermal parameters were set to $1.20U_{eq}$ of the parent non-hydrogen atoms. For compound **I**, the final full-matrix least-squares refinements on F^2 led to R1 = 0.0423 and wR2 = 0.0701 for 2041 observed reflections ($I > 2\sigma(I)$) and 116 variables. The reliability factors for compound **II** (**III**) converged to R1 = 0.0739 (0.0317) and wR2 = 0.0868 (0.0640) for 5091 (675) observed reflections, 396 (29) parameters. The final difference electron density maps showed no features in all cases. Details of unit cell parameters, data collection, and structure refinements are given in Table 1. All computations were performed using the SHELX97 program package.[13] Crystal structure drawings were produced with SCHAKAL 92 and ATOMS, version 5.0.[14]

Thermal Analysis. Differential scanning calorimetry (DSC) measurements were carried out on a computer-controlled TA Instrument DSC-2920 analyzer. Powder samples of **I** (17.000 mg) were sealed into an aluminum pan. An approximately equal mass of sealed empty aluminum pan was used as a reference. The samples were heated at a rate of 5 °C/min from room temperature to 500 °C and then cooled under nitrogen gas current. The residues were examined by powder X-ray diffraction immediately after the DSC experiments.

Diffuse Reflectance Measurements. Optical diffuse reflectance spectrum of **I** was measured at room temperature with a Shimadzu UV-3101PC double-beam, double-monochromator spectrophotometer. Data were collected in the wavelength range 250−2000 nm. $BaSO_4$ powder was used as a standard (100% reflectance). A similar procedure as previously described[15] was used to collect and convert the data using the Kubelka−Munk function.[16] The scattering coefficient (*S*) was treated as a constant because the average particle size of the samples used in the measurements was significantly larger than 5 *μ*m.

Results and Discussion

Synthesis. The syntheses of the title compounds involved complex redox processes in which the oxidation states of the metal ions remained unchanged, while tellurium (Te^{2-} and Te) underwent disproportionation reactions to give rise to $(Te_x)^{2-}$. Although Bi in **I** and Ti in **III** was not incorporated into the final structures, Bi_2Te_3 was found to enhance the crystal growth of **I** and $TiTe_2$ played an important role in the formation of **III.** A separate set of experiments was conducted in ethylenediamine (en) solutions in which only K_2Te, CuCl, and Te were used for the preparation of **III**. Te and CuTe were found to be the main products along with an unknown phase. Direct reactions of a stoichiometric mixture of binary metal−telluride precursors and elemental Te at different temperatures (200 and 300 °C, respectively) for 4 days gave similar results without generating **III**. In contrast, the reaction of a stoichiometric mixture of Rb_2Te, HgTe, and Te in en at 160 °C for 8 days yielded a single-phase polycrystalline sample of **I**.

Physical Properties. Thermal analysis via differential scanning calorimetry (DSC) showed that $Rb_4Hg_5(Te_2)_2(Te_3)_2Te_3$ (**I**) melted incongruently at ca. 200 °C. Examination of the residue by powder XRD revealed that the compound decomposed to HgTe and an unknown amorphous material. The optical spectrum of **I** displays a steep absorption edge with an estimated band gap of 0.8 eV, which suggests that the material is a narrow-gap semiconductor, consistent with its color.

Structure Description. The crystal structure of $Rb_4Hg_5(Te_2)_2(Te_3)_2Te_3$ (**I**) consists of 1D infinite ribbons of $^1_\infty[Hg_5(Te_2)_2(Te_3)_2Te_3]^{4-}$ running along the [010] direction and are separated by Rb^+ cations, as seen in Figure 1. The repeating unit of these ribbons is the pentanuclear metal cluster $[(Hg^{2+})_5(Te_2^{2-})_2(Te_3^{2-})_2(Te^{2-})_3]^{4-}$ (see Figure 2), which has crystallographically imposed *m* symmetry and is composed of four tetrahedral $HgTe_4$

(13) Sheldrick, G. M. *SHELX-97: Program For Structure Refinement*; University of Göttingen: Göttingen, Germany, 1997.
(14) (a) Keller, E. *SCHAKAL 92: A Computer Program for Graphical Representation of Crystallographic Models*; University of Freiburg: Freiburg, Germany, 1992. (b) *ATOMS*, version 5.0 for Windows; Shape Software: Kingsport, TN, 2000.
(15) Li, J.; Chen, Z.; Wang, X.-X.; Proserpio, D. M. *J. Alloys Compounds* **1997**, *262−263*, 28.
(16) Wendlandt, W. WM.; Hecht, H. G. *Reflectance Spectroscopy*; Interscience: New York, 1966.

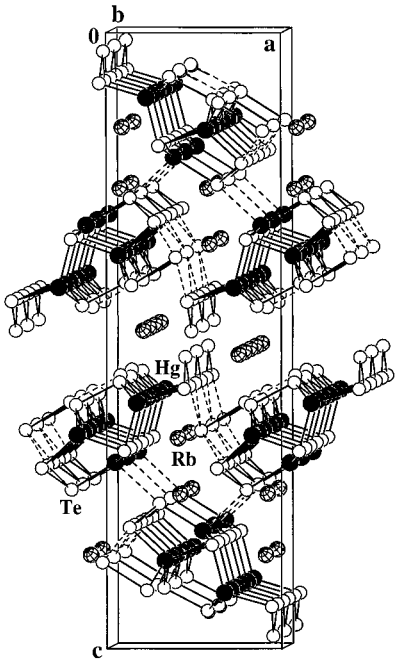

Figure 1. View of $Rb_4Hg_5(Te_2)_2(Te_3)_2Te_3$ (**I**) projected along the *b* axis. Solid circles are Hg, open circles are Te, and doubly shaded circles are Rb. The Hg···Te and Te···Te nonbonding interactions less than 3.6 Å are drawn with dashed lines.

and one trigonal $HgTe_3$ connected through bridging $(Te_2)^{2-}$ and $(Te_3)^{2-}$ and corner-sharing Te. Within the cluster, the five Hg centers are arranged in a distorted square pyramidal geometry, where one $(Te_3)^{2-}$ unit (Te8−Te7−Te8) and two monotelluride Te^{2-} units (Te1) cap three triangular faces of the pyramid and where one $(Te_2)^{2-}$ unit (Te3−Te4) caps its basal plane. The remaining $(Te_3)^{2-}$ unit (Te10−Te9−Te10) acts as a μ_2-type ligand and bonds to the two basal Hg in a trans conformation with respect to the other $(Te_3)^{2-}$ unit (Te8−Te7−Te8). The clusters are interconnected by Te^{2-} (Te2) and $(Te_2)^{2-}$ (Te5−Te6) to form a 1D strand. Note that Te6 atoms do not form any direct bonds with the metal atoms. The μ_4-$(Te_2)^{2-}$ species such as the Te3−Te4 pair are common in polychalcogenide chemistry, as found in $Cs_3Cu_8Te_{10}$,[17] $[NBu_4]_4[Hg_4Te_{12}]$,[18] and $K_2Cu_2(Te_2)(Te_3)$ (**III**), to be discussed below, while the μ_2-$(Te_2)^{2-}$ dangling bond (the Te5−Te6 pair, coordinated to two metal centers via a single Te5) is rare. Limited examples of metal tellurides with bridging μ_2-$(Te_2)^{2-}$ ligands in a dangling mode are $K_4Hf_3Te_{17}$ [19] and $[K\text{-}2,2,2\text{-}crypt]_2[Mo_4(Te_2)_5(Te_3)_2(en)_4]$.[20]

The 1D $^1_\infty[Hg_5(Te_2)_2(Te_3)_2Te_3]^{4-}$ strands are separated by three distinct rubidium cations: Rb1, Rb2, and Rb3. Their coordination with Te atoms is 10 (Rb1), 7 (Rb2), and 7 (Rb3), with an average Rb−Te distance of 3.816 (Rb1), 3.730 (Rb2), and 3.835 (Rb3) Å, respectively. Other selected atomic distances and angles are given in Table 2. The Hg−Te bond distances (2.749(1)−2.957(1) Å) are comparable with the tri- or tetracoordinated Hg found in $Rb_2Hg_3Te_4$ [21] and RbHgSbTe$_3$ (2.69−2.91 Å),[15] and the Te−Te bond distances of 2.747(2)−2.985(2) Å are typical of many polytellurides. $HgTe_4$ tetrahedra are slightly distorted with Te−Hg−Te angles ranging from 99.79(5)° to 120.98(4)° for Hg2 and from 102.69(6)° to 118.02(5)° for Hg3. In contrast, the pseudotrigonal planar $Hg1Te_3$ unit is severely distorted from the ideal trigonal planar geometry, with the three Te−Hg1−Te angles of 2 × 110.49(3)° and 137.67(7)°. The Hg1 atom lies 0.182(2) Å out of the plane formed by three Te atoms, and it is displaced toward the Te7 atom of a neighboring $^1_\infty[Hg_5(Te_2)_2(Te_3)_2Te_3]^{4-}$ strand, forming an additional contact of 3.371(2) Å (see dashed lines in Figure 1), which is less than the sum of the Hg and Te van der Waals radii (3.60 Å), indicating a secondary bonding interaction. Similar weak interactions may also exist among tellurium atoms, as revealed by short intra- and interstrand Te···Te nonbonding contacts of 3.201(3)−3.519(2) Å. A quasi two-dimensional network would result when taking into consideration all Hg−Te and Te−Te contacts shorter than 3.6 Å (as shown in Figure 1 by dashed lines). The van der Waals gaps and channels between and within the layers are filled by the Rb^+ cations.

$[Zn(en)_3]_4In_{16}(Te_2)_4(Te_3)Te_{22}$ (**II**) crystallizes in the monoclinic space group *C*2/*c* with a unusually large unit cell [V = 12 332(4) Å^3] and a complicated layer structure. The primary building blocks in this structure are $InTe_4$ tetrahedra (T1). Four of these $InTe_4$ tetrahedra form a tetrahedral cluster or supertetrahedron In_4Te_{10} (T2), which act as secondary building blocks (Figure 3, top).[22] The T2 clusters share bonds via μ_2-Te (Te11), μ_2-Te_2 (Te5−Te6), and μ_6-Te_3 (Te2−Te1−Te2) to extend into a 2D layered network as shown in Figure 4. Alternatively, the anionic framework can be considered as being built on the $In_{16}Te_{35}$ subunit that features 16 In metal centers arranged into four In_4Te_{10} (or T2) clusters and held together to form a cyclic ring via Te, Te_2, and Te_3 in different bonding modes (Figure 3, bottom). The unusual cyclic $In_{16}Te_{35}$ has a C_2 symmetry, with its 2-fold axis parallel to the [010] direction passing through the central Te1 atom of the Te_3 fragment and its cyclic center axis along the [001] direction (Figure 3). Each cluster ring links to its inversion-center-related partner via two Te3−Te4 bonds within the unit cell, which then extends along the *b* and *c* axes through the μ_2-Te12 and μ_2-(Te3−Te4), respectively, to generate a 2D layer (Figure 4A). These layers stack along the *a* axes with the neighboring layers shifted by ($^1/_2$)*b*. Relatively large pores of approximate dimensions of 8.46 Å × 8.55 Å are found within the layers (Figure 4B). The template cations $[Zn(en)_3]^{2+}$ fill the cavities within and between the layers. The shortest interlayer Te···Te contact is 4.077(4) Å, and the shortest Te···N distance between the anions and cations is 3.60(2) Å. There are two independent $[Zn(en)_3]^{2+}$ ions in the structure; both Zn are 6-fold-coordinated by three chelating en ligands, forming a distorted octahedron. Zn−N distances, 2.12(3)−2.32(3) Å, are in the same range as reported for other $[Zn(en)_3]^{2+}$ complexes.[23] The In−Te bond lengths [2.722(3)−2.935(3) Å] (Table 2) are in good agreement with those observed in $[M(en)_3]In_2Te_6$ (M = Fe, Zn) (2.761(2)−2.825(1) Å)[12] and $[La(en)_4Cl]In_2Te_4$ (2.779(2)−2.787(2) Å),[24] all featuring tetrahedrally coordinated In. Of the 11 independent monotelluride ligands, Te7, Te15, and Te16 are triply bridging and the others are all doubly bridging to the indium atoms. While the two Te_2 function as conventional μ_2-bridging ligands, the coordination of Te_3 is quite unusual. It bridges six indium atoms, with each tellurium atom acting as a μ_2 type (Figure 3, bottom). The Te−Te bond distances in the ditelluride units are normal, at 2.797(3)−2.807(3) Å, while those within the tritelluride units are somewhat

(17) Zhang, X.; Park, Y.; Hogan, T.; Schindler, J. L.; Kannewurf, C. R.; Seong, S.; Albright, T.; Kanatzidis, M. G. *J. Am. Chem. Soc.* **1995**, *117*, 10300.
(18) Haushalter, R. C. *Angew. Chem., Int. Ed. Engl.* **1985**, *24*, 433.
(19) Keane, P. M.; Ibers, J. A. *Inorg. Chem.* **1991**, *30*, 1327.
(20) Eichhorn, B. W.; Haushalter, R. C.; Cotton, F. A.; Wilson, B. *Inorg. Chem.* **1988**, *27*, 4084.
(21) Li, J.; Chen, Z.; Lam, K.-C.; Mulley, S.; Proserpio, D. M. *Inorg. Chem.* **1997**, *36*, 684.
(22) Li, H.-Y.; Laine, A.; O'Keeffe, M.; Yaghi, O. M. *Science* **1999**, *283*, 1145.

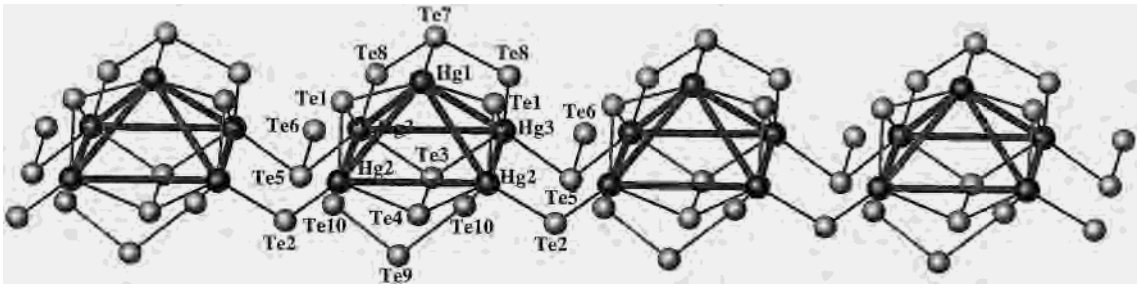

Figure 2. Fragment of the $^{1}_{\infty}[Hg_5(Te_2)_2(Te_3)_2Te_3]^{4-}$ anionic ribbon with the atomic labeling scheme. The Hg_5 square pyramids are outlined.

Table 2. Selected Bond Lengths (Å) and Angles (deg) for $Rb_4Hg_5(Te_2)_2(Te_3)_2Te_3$ (**I**), $[Zn(en)_3]_4In_{16}(Te_2)_4(Te_3)Te_{22}$ (**II**), and $K_2Cu_2(Te_2)(Te_3)$ (**III**)

Compound **I**			
Hg(1)−Te(1)	2.749(1) × 2	Te(1)−Hg(1)−Te(1)	137.67(7)
Hg(1)−Te(7)	2.886(2)	Te(1)−Hg(1)−Te(7)	110.49(3) × 2
Hg(1)−Te(7)	3.371(2)	Te(10)−Hg(2)−Te(1)	120.98(4)
Hg(2)−Te(10)	2.775(1)	Te(10)−Hg(2)−Te(2)	114.31(5)
Hg(2)−Te(1)	2.798(2)	Te(1)−Hg(2)−Te(2)	108.66(5)
Hg(2)−Te(2)	2.817(2)	Te(10)−Hg(2)−Te(4)	99.79(5)
Hg(2)−Te(4)	2.957(1)	Te(1)−Hg(2)−Te(4)	106.32(5)
Hg(3)−Te(8)	2.747(2)	Te(2)−Hg(2)−Te(4)	104.80(5)
Hg(3)−Te(1)	2.793(1)	Te(8)−Hg(3)−Te(1)	118.02(5)
Hg(3)−Te(5)	2.814(2)	Te(8)−Hg(3)−Te(5)	102.69(6)
Hg(3)−Te(3)	2.929(1)	Te(1)−Hg(3)−Te(5)	116.20(5)
Te(3)−Te(4)	2.747(2)	Te(8)−Hg(3)−Te(3)	105.22(5)
Te(5)−Te(6)	2.941(3)	Te(1)−Hg(3)−Te(3)	107.06(5)
Te(7)−Te(8)	2.985(2) × 2	Te(5)−Hg(3)−Te(3)	106.68(5)
Te(9)−Te(10)	2.808(2) × 2	Te(8)−Te(7)−Te(8)	96.81(8)
		Te(10)−Te(9)−Te(10)	104.17(8)
Compound **II**			
In(1)−Te(10)	2.727(3)	In(5)−Te(14)	2.779(3)
In(1)−Te(8)	2.745(2)	In(5)−Te(16)	2.849(3)
In(1)−Te(7)	2.807(3)	In(6)−Te(11)	2.726(3)
In(1)−Te(1)	2.935(3)	In(6)−Te(13)	2.768(3)
In(2)−Te(3)	2.722(3)	In(6)−Te(6)	2.776(3)
In(2)−Te(8)	2.756(3)	In(6)−Te(15)	2.851(3)
In(2)−Te(2)	2.796(3)	In(7)−Te(17)	2.729(2)
In(2)−Te(7)	2.826(3)	In(7)−Te(14)	2.770(3)
In(3)−Te(11)	2.744(3)	In(7)−Te(15)	2.819(3)
In(3)−Te(9)	2.758(3)	In(7)−Te(16)	2.859(3)
In(3)−Te(5)	2.759(3)	In(8)−Te(4)	2.740(3)
In(3)−Te(7)	2.854(3)	In(8)−Te(17)	2.746(3)
In(4)−Te(10)	2.734(3)	In(8)−Te(15)	2.823(3)
In(4)−Te(9)	2.757(3)	In(8)−Te(16)	2.833(3)
In(4)−Te(12)	2.771(3)	Te(1)−Te(2)	3.006(2) × 2
In(4)−Te(2)	2.836(3)	Te(3)−Te(4)	2.807(3)
In(5)−Te(12)	2.736(3)	Te(5)−Te(6)	2.797(3)
In(5)−Te(13)	2.758(3)	Te(2)−Te(1)−Te(2)	172.4(1)
Compound **III**			
Cu−Te(2)	2.593(2)	Te(2)−Cu−Te(1)	112.75(3) × 2
Cu−Te(1)	2.6538(9) × 2	Te(1)−Cu−Te(1)	114.81(5)
Cu−Te(2)	2.655(2)	Te(2)−Cu−Te(2)	102.84(5)
Cu−Cu	2.574(3)	Te(1)−Cu−Te(2)	106.24(3) × 2
Te(1)−Te(1)	2.798(1)	Te(2)−Te(3)−Te(2)	103.06(4)
Te(3)−Te(2)	2.781(1) × 2		

longer (3.006(2) Å) compared to the typical Te−Te covalent bond distance (2.69−2.80 Å). Band structure calculations on $BaBiTe_3$ have shown that a Te−Te distance of 3.098(2) Å corresponds to a weak Te−Te bonding interaction.[25] For **II**, by use of Paulings's rule [$d(n) = d(1) - 0.61 \log(n)$, $d(1) = 2.796$ Å],[26] a formal bond order of 0.45 can be computed for the Te−Te in Te_3, confirming their bonding characteristics. This is further reflected by the formal oxidation state assignment, which gives an average valence of $-4/3$ for each Te atom of the Te_3 unit if Zn^{2+}, In^{3+}, ditelluride $(Te_2)^{2-}$, and monotelluride Te^{2-} were assumed. The material is expected to be a metallic conductor, although an actual conductivity measurement has not been carried out because of the difficulties in obtaining a single-phased sample.

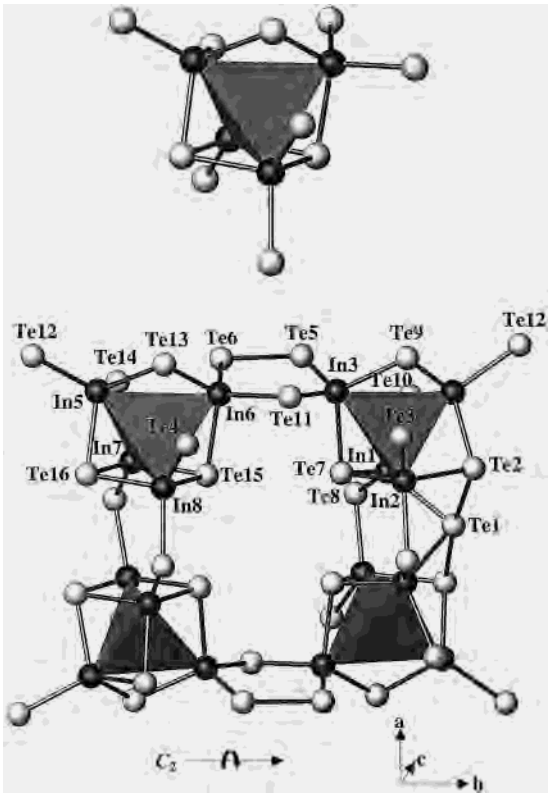

Figure 3. View of the In_4Te_{10} supertetrahedron (T2) (top) and the $In_{16}Te_{35}$ fragment (bottom) found in $[Zn(en)_3]_4In_{16}(Te_2)_4(Te_3)Te_{22}$ (**II**) shown approximately down the *c* axis. The 2-fold symmetry rotation axis (C_2) is indicated in the figure. Light-colored circles are Te atoms, and dark circles are In atoms.

The crystal structure of $K_2Cu_2(Te_2)(Te_3)$ (**III**) contains $CuTe_4$ tetrahedra that are linked by intralayer $(Te_3)^{2-}$ and interlayer $(Te_2)^{2-}$ units to give rise to a 3D network (Figure 5), with the K^+ cations located in the cavities. As seen in Figure 6, within each layer, the Cu atoms are paired up, giving a Cu−Cu distance of 2.574(3) Å. The two Cu atoms in the pair are also bridged by a μ_2-Te_3 (Te2−Te3 = 2.781(1) Å, Te2−Te3−Te2 = 103.06(4)°), thereby forming a Cu_2Te_3 five-membered ring. Each Cu_2Te_3 ring is connected to four others in a centered arrangement through the inter-ring Cu−Te2 bonds, leading to the overall $[Cu_2Te_3]$ 2D network. The 2D net, which can also be viewed as being composed of fused five-membered Cu_2Te_3 and nine-membered Cu_4Te_5 rings, is situated on the mirror planes in the orthorhombic (*Cmcm*) structure and is therefore completely flat. Applying the *c*-glide symmetry operator to the net at $z = 0.25$ produces the adjacent equivalent nets above and below, at $z = 0.75$ and -0.25, respectively. These planar nets are held together by the $(Te_2)^{2-}$ dimeric units, which complete the

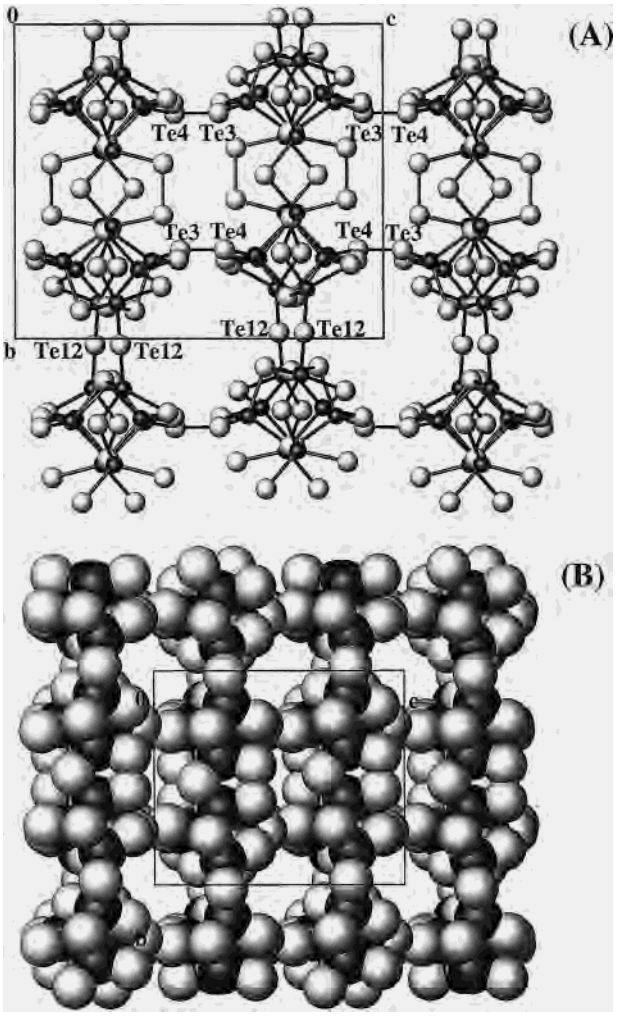

Figure 4. (A) Projection of the $^{2}_{\infty}[In_{16}(Te_2)_4(Te_3)Te_{22}]^{8-}$ anionic layer along the monoclinic *a* axis. (B) Space-filling plot of the same anionic layer to show the cavities. The same labeling scheme as in Figure 3 is used here.

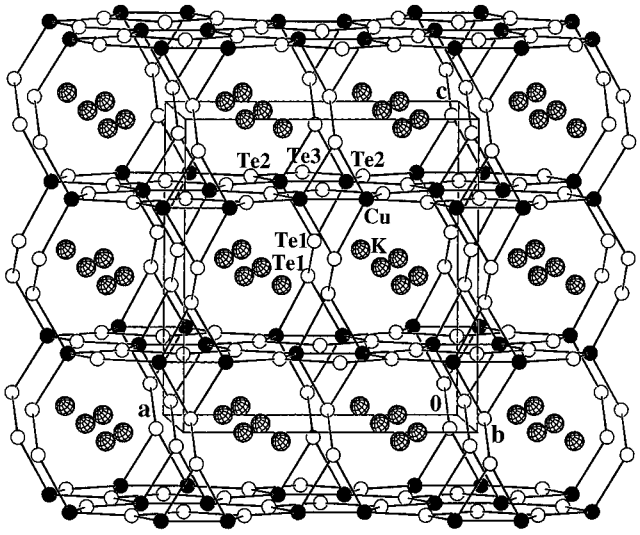

Figure 5. The 3D framework of $K_2Cu_2(Te_2)(Te_3)$ (**III**) projected along the *b* axis. Solid circles are Cu, open circles are Te, and doubly shaded circles are K.

tetrahedral coordination sphere of the Cu atoms and form a 3D $^{3}_{\infty}[Cu_2(Te_2)(Te_3)]^{2-}$ network (see Figure 5). Each $(Te_2)^{2-}$ functions as a μ_4 ligand, linking two Cu atoms from the net above and the other two Cu from the net below. The Te1−Te1 bond of 2.798(1) Å lies in the crystallographic *bc* plane, making an angle of 57.05° with the *c* axis. As a result, open channels are formed along the *b* axis by enclosing the neighboring planes and the $(Te_2)^{2-}$ units. The approximate dimensions of the hexagon-shaped cross section of the channels are 5.7 Å × 5.9 Å (Figure 5). Similar channels with an irregular-shaped cross section of ca. 5.6 Å × 6.0 Å are also formed running parallel to the [110] direction. Two rows of K^+ cations reside in the channels, and each K^+ ion is 10-coordinate to tellurium in a bicapped square antiprismatic geometry, with K−Te distances of 3.6025(6)−3.796(2) Å, which agrees well with those observed in $K_4Cu_8Te_{11}$ (average 3.66(23) Å).[27] The $CuTe_4$ tetrahedra are distorted with Cu−Te distances ranging from 2.593(2) to 2.655(2) Å and Te−Cu−Te angles of 102.84(5)−114.81(5)° (Table 2). The shortest Cu−Te distances are those within the Cu_2Te_3 rings, and the longest ones are associated with the inter-ring Cu−Te2 bonds. The short Cu−Cu contact of 2.574(3) Å lies close to the lower end of those found for this class of compounds, such as 2.561(2) Å in $K_{1.5}Dy_2Cu_{2.5}Te_5$,[28] 2.649−2.674 Å in $Cu_2SbSe_3 \cdot x(en)$, $x = 0.5, 1$,[29] and 2.678−2.784 Å in $Cs_2Cu_2Sb_2Se_5$.[30]

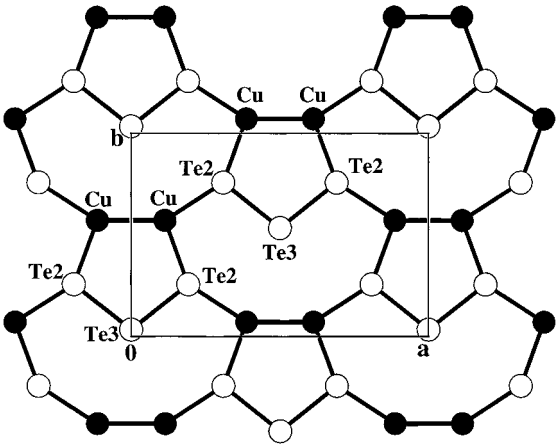

Figure 6. Projection of the Cu_2Te_3 2D net along the [001] direction (*c* axis). The same labeling scheme as in Figure 5 is used here.

$Rb_4Hg_5(Te_2)_2(Te_3)_2Te_3$ (**I**), $[Zn(en)_3]_4In_{16}(Te_2)_4(Te_3)Te_{22}$ (**II**), and $K_2Cu_2(Te_2)(Te_3)$ (**III**) represent three different new extended structure types, and they are rare examples of the ternary polytellurides containing both Te_2 and Te_3 fragments that are obtained by solvothermal methods using en as a reaction medium. The only other polytellurides containing Te_3 that are prepared via the same routes are $[M(en)_3]Hg_2(Te_2)(Te_3)_2Te$ (M = Fe, Mn),[31] which are typical examples of tellurometalates.[32] In addition, $[Zn(en)_3]_4In_{16}(Te_2)_4(Te_3)Te_{22}$ (**II**) also represents

(23) Cernak, J.; Chomic, M. D.-J.; Kappenstein, C. *Inorg. Chim. Acta* **1984**, *85*, 219.
(24) Li, J.; Chen, Z.; Chen, F.; Proserpio, D. M. *Inorg. Chim. Acta* **1998**, *273*, 255.
(25) Chung, D.-Y.; Jobic, S.; Hogan, T.; Kannewurf, C. R.; Brec, R.; Rouxel, J.; Kanatzidis, M. G. *J. Am. Chem. Soc.* **1997**, *119*, 2505.
(26) Pauling, L. *The Chemical Bond*; Cornell University Press: Ithaca, New York, 1976.
(27) Park, Y.; Kanatzidis, M. G. *Chem. Mater.* **1991**, *3*, 781.
(28) Huang, F. Q.; Choe, W.; Lee, S.; Chu, J. S. *Chem. Mater.* **1998**, *10*, 1320.
(29) Chen, Z.; Dilks, R. E.; Wang, R.-J.; Li, J. *Chem. Mater.* **1998**, *10*, 3184.
(30) Chen, Z.; Wang, R.-J.; Dilks, K. J.; Li, J. *J. Solid State Chem.* **1999**, *147*, 132.
(31) Li, J.; Rafferty, B. G.; Mulley, S.; Proserpio, D. M. *Inorg. Chem.* **1995**, *34*, 6417.
(32) Ansari, M. A.; McConnachie, J. M.; Ibers, J. A. *Acct. Chem. Res.* **1993**, *26*, 574.

one of the few examples of 2D structures containing large metal−en complexes. The only known layered compounds of this kind are $[Ga(en)_3]In_3Te_7$,[4] $[Co(en)_3]CoSb_4S_8$,[33] and $[Mn(en)_3]Ag_6Sn_2Te_8$.[34] The most common coordination of Te_3 is the μ_2 type with the metals bonded to terminal Te atoms, as observed in the Te10−Te9−T10 of **I** and Te2−Te3−Te2 of **III**. Direct coordination of the central Te atom of the Te_3 unit, as that of the μ_3-Te8−Te7−Te8 in **I** and μ_6-Te2−Te1−Te2 in **II**, is quite rare. The unusual 6-fold-coordinated μ_6-$(Te_3)^{3-}$ unit has been found in the structure of $(Et_4N)_4[Au(Ag_{1-x}Au_x)_2Sn_2Te_9]$ ($x = 0.32$) (synthesized from solvent extraction of intermetallic alloys),[35] whereas the μ_3-$(Te_3)^{2-}$ in **I**, to the best of our knowledge, represents a new bridging mode of a tritelluride unit reported thus far.

Acknowledgment. The authors thank the National Science Foundation for its generous support through Grant DMR-9553066.

Supporting Information Available: Four X-ray crystallographic files, in CIF format. This material is available free of charge via the Internet at http://pubs.acs.org.

IC000648C

(33) Stephan, H.-O.; Kanatzidis, M. G. *J. Am. Chem. Soc.* **1996**, *118*, 122.
(34) Chen, Z.; Wang, R.-J.; Li, J. *Chem. Mater.* **2000**, *12*, 762.
(35) Dhingra, S. S.; Seo, D.-K.; Kowach, G. R. *Angew. Chem., Int. Ed. Engl.* **1995**, *36*, 1087.